

# Finite-Temperature Quarkyonic Matter

## with an Excluded Volume Model for Nuclear Interactions

Srimoyee Sen\*

*Department of Physics and Astronomy,  
Iowa State University, Ames, IA 50011-3160*

Neill C. Warrington†

*Institute for Nuclear Theory, University of Washington, Seattle, Washington 98195-1550*

### Abstract

We compute finite temperature properties of a recently proposed “excluded volume” model of quarkyonic matter under thermodynamic conditions found in binary neutron star mergers. To do so, we extend this model by introducing finite temperature distribution functions and entropy functionals. The main effect of temperature is to decrease by a small amount the baryon density at which the quarkyonic phase emerges, and to increase the density of quarks produced. To the extent this model describes reality, we conclude that hot environments such as neutron star mergers are more likely to host deconfined quark matter than their zero temperature counterparts.

---

\* [srimoyee08@gmail.com](mailto:srimoyee08@gmail.com)

† [ncwarrin@uw.edu](mailto:ncwarrin@uw.edu)

## I. INTRODUCTION

Quarkyonic matter is a proposed phase of intermediate density QCD at large  $N_c$  where confinement persists [1]. In this phase, baryons form a degenerate fermi gas where the total baryon number is distributed among both quark and nucleon degrees of freedom. One postulated feature of quarkyonic matter [1, 2] that sets it apart from other mixed quark-nucleon phases is the structure of the momentum space distribution function. At zero temperature, due to confining forces at the fermi surface, the momentum space distribution consists of an inner sphere of quarks surrounded by an outer shell of nucleons. Compared with models exhibiting first order phase transitions [3, 4], this shell structure produces a stiff equation of state at moderate densities, while retaining a soft equation of state at lower densities, making quarkyonic matter attractive for neutron star phenomenology [5–7].

It was recently shown [5] that a pronounced peak in the speed of sound of nuclear matter, expected from neutron star observations [8], is reproduced by a model of quarkyonic matter. In this model, the momentum space shell structure is imposed through particular choices of quark and nucleon distribution functions. Interestingly, these distribution functions arise naturally in a simple model capturing some essential features of QCD, where quarks are treated as free particles and nucleons interact with each other via hard core repulsion [7]. We will refer to this model as the “excluded volume” model of quarks and nucleons for the rest of the paper. Minimizing the total energy density of this two-component model yields a hadronic phase at low total baryon density and a quarkyonic phase at high baryon density, with the momentum space shell structure of [5] emerging dynamically. In this paper we extend this excluded volume model to finite temperature.

Probing the existence of quark matter through binary neutron star mergers motivates our analysis [9]. Recently it has become evident that information about the phase of matter present may be contained in the post-merger signal [3, 10], and some questions which may be addressed are: whether neutron stars have deconfined quark matter in their cores [9], and whether there is a phase transition between hadronic and quark degrees of freedom [11]. Reaching temperatures on the order of 50 MeV [12], however, neutron star mergers present new theoretical challenges. Most *ab-initio* methods in nuclear physics are designed for zero temperature systems [13–15], and analyzing mergers with lattice QCD is currently not practical due to the sign problem [16]. In absence of an exact method, few model

calculations of finite temperature dense matter have been performed [11]. The primary goal of this paper, therefore, is to contribute to these few studies by extending the excluded volume model of quarkyonic matter model to finite temperatures. Within the model, we calculate the quark-onset density under thermodynamic conditions found in neutron star mergers. We find the effect of raising the temperature, though small, is to favor quark production.

This paper is organized as follows. In Sec. II we will define the excluded volume model at zero-temperature. In Sec. III we extend the model to finite temperature and in Sec. IV we present our findings. Finally, we conclude in Sec. V.

## II. EXCLUDED VOLUME MODEL AT $T = 0$

In this section we review the zero temperature ( $T = 0$ ) excluded volume model. In particular, we show how the distribution function of baryons evolves from purely nucleonic to quarkyonic as the baryon density is increased. For simplicity, throughout this paper we will consider isospin symmetric matter.

The central idea of quarkyonic matter is that confinement persists even at high baryon density [1]. Due to confining forces, quarks near the edge of the Fermi sea bind together to produce nucleons, while quarks deep within the Fermi sea, being Pauli blocked, do not. These considerations lead to a momentum space “shell structure”, depicted in Fig. 1, where high density matter is supposed to be a fermi sphere of free quarks surrounded by a fermi shell of nucleons.

While the existence of quarkyonic matter cannot currently be deduced from first principle calculations in QCD, the excluded volume model of [7] generates the shell structure dynamically at zero temperature. The excluded volume model includes both nucleons and quarks as degrees of freedom, with quarks treated as free particles and nucleons interacting via hard-core repulsion. The hard-core repulsion is modeled by assigning each nucleon a volume  $v_0$ , so that  $N$  nucleons in volume of  $V$  can only access a volume of  $V - Nv_0$ . This implementation of repulsive forces is perhaps crude, however such forces do exist, as can be deduced from partial wave analyses [17], chiral effective field theory [18], or simply by the fact that nuclei exist. In addition to producing the shell structure, the excluded volume theory predicts sensible low and high density limits: at low baryon density one obtains a

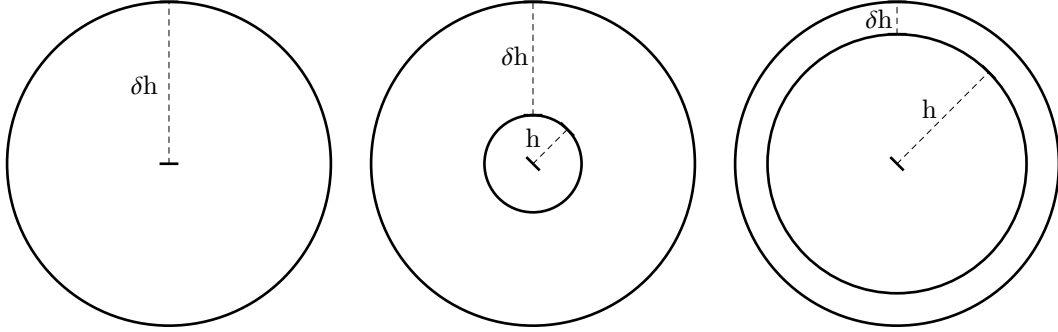


FIG. 1: Here we depict two-dimensional projections of the momentum space shell structure of quarkyonic matter at a variety of total baryon number densities, increasing from left to right. At low density, the system is composed entirely of nucleons, resulting in a momentum space distribution which is all “shell”, with radius  $\delta h$ . Increasing the density, an inner fermi surface of quarks with radius  $h$  is produced. The inner fermi sphere grows with density, leading eventually to a thin shell of nucleons in momentum space.

dilute gas of nucleons, and at high density a dense gas of quarks.

To implement the model, note that both quarks and nucleons contribute to the total baryon number density:

$$n_{tot} = n_N + n_Q . \quad (1)$$

Here  $n_{tot}$  is the total baryon number density, and  $n_N$  and  $n_Q$  are the baryon number density in nucleons and quarks, respectively [19]. Related to  $n_N$  and  $n_Q$  are the energy density in nucleons and quarks,  $\epsilon_N$  and  $\epsilon_Q$ . According to the laws of thermodynamics [20], at zero temperature the equilibrium configuration is obtained by minimizing the total energy density

$$\epsilon_{tot} = \epsilon_N + \epsilon_Q \quad (2)$$

at fixed total baryon density. The equilibrium configuration of the system is fully specified through this minimization procedure when  $\epsilon_N(n_N)$  and  $\epsilon_Q(n_Q)$  are supplied. In the excluded volume model, these dependencies are supplied through intermediary quantities, namely the distribution functions of quarks and nucleons, which we denote as  $f_Q(k)$  and  $f_N(k)$ , and take to be:

$$\begin{aligned} f_Q(k) &= \theta(h/N_c - \epsilon_Q(k)) \\ f_N(k) &= \theta(h + \delta h - \epsilon_N(k))\theta(\epsilon_N(k) - h) . \end{aligned} \quad (3)$$

These definitions implement a fermi sphere of quarks surrounded by a shell of nucleons. The baryon density in quarks  $n_Q$  and the baryon density in nucleons  $n_N$  are defined as the following functionals of  $f_Q$  and  $f_N$  [7]:

$$\begin{aligned} n_Q &= N_f(2s+1) \int \frac{d^3k}{(2\pi)^3} f_Q(k) \\ \frac{n_N}{1-n_N/n_0} &= N_f(2s+1) \int \frac{d^3k}{(2\pi)^3} f_N(k) , \end{aligned} \quad (4)$$

as are the energy densities:

$$\begin{aligned} \epsilon_Q &= N_c N_f(2s+1) \int \frac{d^3k}{(2\pi)^3} f_Q(k) \epsilon_Q(k) \\ \frac{\epsilon_N}{1-n_N/n_0} &= N_f(2s+1) \int \frac{d^3k}{(2\pi)^3} f_N(k) \epsilon_N(k) . \end{aligned} \quad (5)$$

Here  $\epsilon_Q(k)$  and  $\epsilon_N(k)$  are free quark and nucleon dispersion relations,  $n_0 \equiv v_0^{-1}$  is the hard-core density,  $N_f = 2$  and  $s = 1/2$  is the spin of a quark or nucleon. We neglect throughout this paper anti-particle contributions to all thermodynamic quantities, as they are suppressed by powers of the vanishingly small quantity  $e^{-2M/T}$ . Equations 3-5, along with the minimization procedure, fully define the excluded volume model at zero temperature.

For intuition of how the model might capture the properties of high density matter, note that baryon number can be stored either in quark degrees of freedom or nucleon degrees of freedom. No particular configuration is enforced, and which degrees of freedom are actually present in equilibrium at a given density is determined by the energy cost. This is depicted schematically in Fig. 2.

We now demonstrate that the excluded volume theory generates quarkyonic matter. To proceed, we must specify the dispersion relations of the quarks and nucleons. Throughout this paper we employ non-relativistic dispersion relations:

$$\begin{aligned} \epsilon_Q(k) &= m + \frac{k^2}{2m} \\ \epsilon_N(k) &= M + \frac{k^2}{2M} , \end{aligned} \quad (6)$$

where  $M$  is the nucleon mass and  $m$  is the quark mass with  $m \equiv M/N_c$ . These dispersion relations well-approximate the full relativistic dispersion relations in neutron stars and neutron star mergers, where the density spans the range  $0 \lesssim n/n_{sat} \lesssim 5$  [12, 21]; here  $n_{sat} \equiv 0.16 \text{ fm}^{-3}$  is nuclear saturation density. Indeed, only at  $n/n_{sat} \sim 10$  (for nucleons)

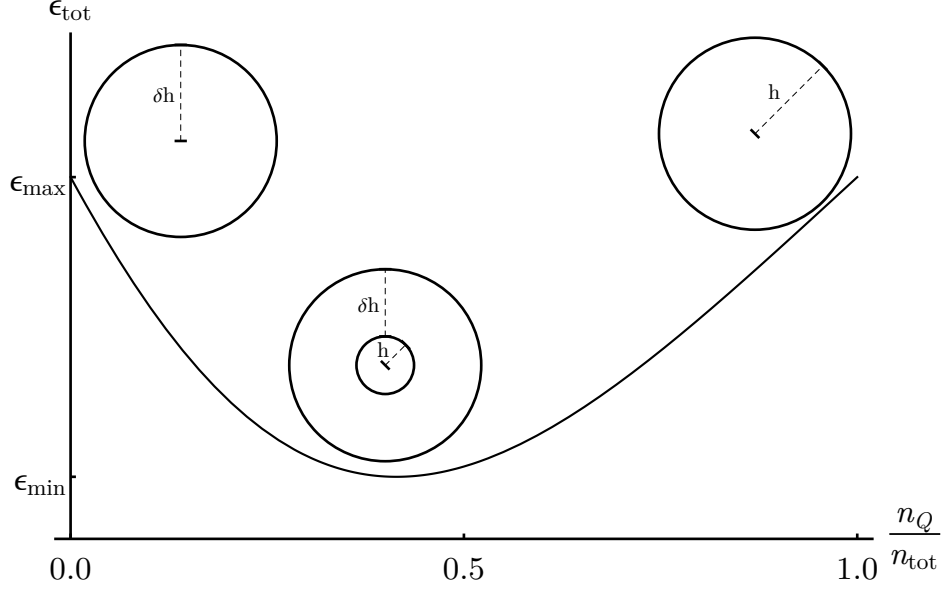


FIG. 2: Here we schematically depict the energy minimization procedure. The horizontal axis is the fraction of baryon density in quarks, and the vertical axes is the total energy density for a given quark fraction. The width of the shell varies as the quark fraction is varied. The system's equilibrium state is that which minimizes the total energy density.

and  $n/n_{sat} \sim 3 - 5$  (for quarks) does the non-relativistic expansion begin to break down. With these specifications,

$$n_Q = N_f(2s+1) \int_0^{\sqrt{2m(h/N_c-m)}} \frac{d^3k}{(2\pi)^3}$$

$$\frac{n_N}{1-n_N/n_0} = N_f(2s+1) \int_{\sqrt{2M(h-M)}}^{\sqrt{2M(h+\delta h-M)}} \frac{d^3k}{(2\pi)^3}, \quad (7)$$

and

$$\epsilon_Q = N_f(2s+1) \int_0^{\sqrt{2m(h/N_c-m)}} \frac{d^3k}{(2\pi)^3} \left( m + \frac{k^2}{2m} \right)$$

$$\frac{\epsilon_N}{1-n_N/n_0} = N_f(2s+1) \int_{\sqrt{2M(h-M)}}^{\sqrt{2M(h+\delta h-M)}} \frac{d^3k}{(2\pi)^3} \left( M + \frac{k^2}{2M} \right). \quad (8)$$

The total energy density is then given by

$$\epsilon_{tot} - Mn_{tot} = N_f(2s+1) \left[ \int_0^{\sqrt{2m(\mu/N_c-m)}} \frac{d^3k}{(2\pi)^3} \frac{k^2}{2m} + (1-n_N/n_0) \int_{\sqrt{2M(\mu-M)}}^{\sqrt{2M(\mu+\delta\mu-M)}} \frac{d^3k}{(2\pi)^3} \frac{k^2}{2M} \right]. \quad (9)$$

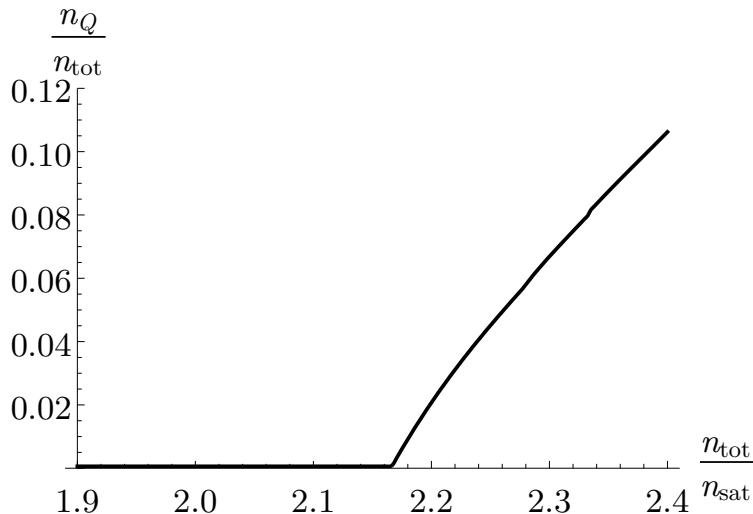


FIG. 3: Here we plot the equilibrium quark fraction  $n_Q/n_{tot}$  as a function of total baryon density. At low density, only nucleons are found in the system while at high densities quarks begin to be produced.

The  $Mn_{tot}$  term is produced by the combined contributions of the rest mass energy from quarks and nucleons, and does not affect a minimization at fixed  $n_{tot}$ . We therefore drop the rest mass contribution in all subsequent calculations. It is straightforward to numerically compute the integrals above, then minimize the total energy at fixed  $n_{tot}$ . Following this procedure results in Fig. 3, where we have taken the hard core density to be  $n=2.5n_{sat}$  (which is about the density of a proton). Here it is seen that the excluded volume model dynamically produces quarkyonic matter: at low density the system is composed of all nucleons, but around the hard-core density quarks are dynamically produced.

Due to the presence of the two fermi surfaces, however, seeing this behavior analytically is complicated. To understand the quark onset behavior, it pays to look at two limiting cases: all nucleons or all quarks. In either of these cases, the two fermi surfaces collapse to one, simplifying expressions. For a given total baryon density  $n_{tot}$ , the energy of an all quark configuration is

$$\epsilon_Q = \frac{1}{5\pi^2 M} N_c^2 \left( \frac{3\pi^2 n_{tot}}{2} \right)^{5/3}. \quad (10)$$

while the energy of an all nucleon configuration is

$$\epsilon_N = \frac{1}{5\pi^2 M} \left( \frac{3\pi^2 n_{tot}}{2} \right)^{5/3} \frac{1}{(1 - n_{tot}/n_0)^{2/3}}. \quad (11)$$

These are qualitatively different behaviors, and account for the general features of Fig. 3. At low density, when  $n_{tot} \ll n_0$ , the energy required to produce quarks is roughly  $N_c^2$  times the energy needed to produce baryons. This is why at low densities the equilibrium configuration consists of all nucleons. However, the energy required to produce nucleons increases with density due to the repulsive interactions, and when

$$(1 - n_{tot}/n_0)^{2/3} \sim N_c^2 \quad (12)$$

nucleons become more difficult to produce than quarks. At this point, the density of nucleons saturate, while quarks are produced in ever greater amount.

### III. EXCLUDED VOLUME MODEL AT $T \neq 0$

We now proceed to the  $T \neq 0$  case. In order to capture thermal effects, we first modify the distribution functions  $f_Q$  and  $f_N$ . We define the finite temperature distribution functions to be the following:

$$\begin{aligned} f_Q(k) &= g(\epsilon_Q(k), \frac{h + \delta h}{N_c}) \theta(h/N_c - \epsilon_Q(k)) \\ f_N(k) &= g(\epsilon_N(k), h + \delta h) \theta(\epsilon_N(k) - h) \end{aligned} \quad (13)$$

where  $g$  is the Fermi-Dirac distribution

$$g(\epsilon, \mu) = \frac{1}{e^{\beta(\epsilon - \mu)} + 1}, \quad (14)$$

and  $\beta = T^{-1}$ . These distribution functions are plotted in Fig. 4 for a visual aid. The density and energy density functionals are still taken to be Eqs. 4 and 5, but are now computed with the distribution functions Eq. 13.

This choice of  $f_Q$  and  $f_N$ , with a common envelope  $g$ , implements both the shell structure (through the  $\theta$  functions) and the observation that there is just one underlying distribution function in quarkyonic matter. Since there is just one outermost fermi surface, heating the system by a small amount should result in a deformation only at this edge (at  $h + \delta h$ ). One feature which is evident from Fig. 4 is that nucleons are affected by temperature before quarks. In the following section we will see this feature produces particular dynamics

An additional new feature enters the finite temperature theory. At  $T \neq 0$  and fixed baryon density, it is the Helmholtz free energy, rather than the energy, which is minimized



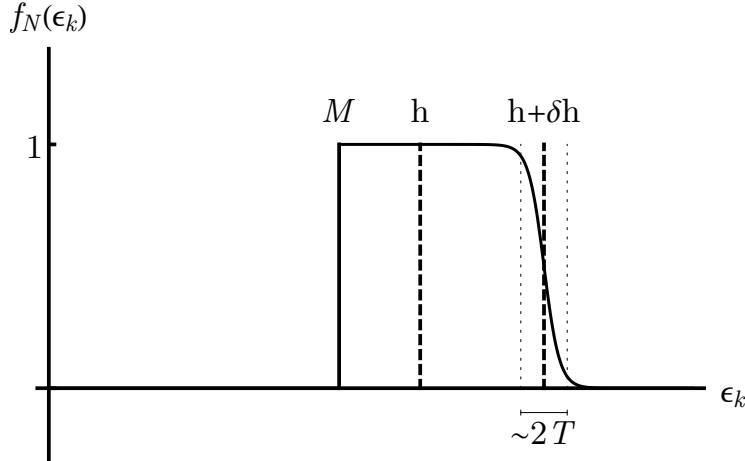


FIG. 4: Here we plot the distribution functions defined in Eq. 13 as a function of energy. Support begins for the distribution function begins at  $M$  and persists until roughly  $h + \delta h$  where the fermi surface is smeared out over a width of order  $T$ . The energy band  $M \leq \epsilon \leq h$  encodes the quark distribution, while the band  $h \leq \epsilon \leq h + \delta h$  encodes the nucleon distribution.

in equilibrium. Since the Helmholtz free energy  $F$  is related to the energy  $E$  by  $F = E - TS$  ( $S$  is the entropy and  $T$  is the temperature) entropy functionals are needed in order to proceed. We define the entropy functionals for quarks ( $s_Q$ ) and nucleons ( $s_N$ ) to be the following:

$$s_Q = N_f N_c (2s + 1) \int \frac{d^3 k}{(2\pi)^3} \theta(h/N_c - \epsilon_Q(k)) \left[ \beta \xi_Q(k) f_Q(k) + \ln(1 + e^{-\beta \xi_Q(k)}) \right]$$

$$\frac{s_N}{1 - n_N/n_0} = N_f (2s + 1) \int \frac{d^3 k}{(2\pi)^3} \theta(\epsilon_N(k) - h) \left[ \beta \xi_N(k) f_N(k) + \ln(1 + e^{-\beta \xi_N(k)}) \right] \quad (15)$$

where  $\xi_Q(k) = \epsilon_Q(k) - (h + \delta h)/N_c$  and  $\xi_N(k) = \epsilon_N(k) - (h + \delta h)$ . To understand this choice of  $s_Q$  and  $s_N$ , recall that the excluded volume model consists of  $N_c$  species of free quarks within the fermi sea, on top of which is a fermi shell of nucleons whose interactions are completely encoded by an excluded volume (i.e the nucleons are free within the excluded volume). Our aim is to implement precisely these observations. Given that the entropy density for a single species for free fermion is

$$s = -\frac{1}{V} \frac{\partial F}{\partial T} = \int \frac{d^3 k}{(2\pi)^3} \left[ \beta(\epsilon(k) - \mu) f(k) + \ln(1 + e^{-\beta(\epsilon(k) - \mu)}) \right], \quad (16)$$

where  $f(k)$  is the Fermi-Dirac distribution, we see that the proposed  $s_Q$  and  $s_N$  describe the entropy of free fermions with the shell structure imposed. The remaining factors in  $s_Q$  and

$s_N$  account for powers of  $N_c$  and the fact that nucleons interact in an excluded volume.

We conclude this section by describing our method for computing the equilibrium properties of the finite temperature excluded volume model. The goal is to find, given a fixed total baryon density, the distribution functions  $f_Q$  and  $f_N$  which minimize the Helmholtz free energy density. Once these functions are known, all thermodynamic quantities can be computed. To accomplish this goal, first a total density  $n_{tot}$  is chosen, and is partitioned into  $n_Q$  and  $n_N$  such that  $n_Q + n_N = n_{tot}$ . Next, the density functionals Eq. 4 are inverted numerically to produce  $h$  and  $\delta h$ . These parameters are then used to compute the energy and entropy densities (Eq. 5 and Eq. 15). This procedure is repeated over all partitions. Minimizing the free energy density, the equilibrium values of  $h$  and  $\delta h$  (and hence the distribution functions) are obtained.

#### IV. RESULTS

In this section we present our findings. We focus on the effect of temperature on quark production. In particular, we compute the onset density of quarks as a function of temperature as well, as the equilibrium quark fraction. We first employ a low-temperature expansion [22], where the expansion parameter is  $\frac{T}{n_{tot}^{2/3}/M}$ , to understand thermal effects analytically. The low temperature expansion suggests that heating the system aids in quark production. Relative to the zero temperature case, heating the system reduces the onset density and raises the fraction of quarks present in equilibrium. We then elaborate upon these analytic arguments with numerical calculations.

In the following we compute the thermodynamic functionals for all quark and all nucleon configurations. We first compute in terms of the shell radii  $h$ ,  $\delta h$  and the temperature  $T$  to lowest non-trivial order in the low temperature expansion, then invert to express the free energy as a function of density. As in the zero temperature case, we drop the rest mass contribution from both the quark and nucleon energy densities. For the nucleons:

$$\begin{aligned} \frac{n_N}{1 - n_N/n_0} &= (2s + 1)N_f \frac{(2M\delta h)^{3/2}}{6\pi^2} \left[ 1 + \frac{\pi^2}{8} \left( \frac{T}{\delta h} \right)^2 \right] \\ \frac{\epsilon_N}{1 - n_N/n_0} &= (2s + 1)N_f \delta h \frac{(2M\delta h)^{3/2}}{10\pi^2} \left[ 1 + \frac{5\pi^2}{8} \left( \frac{T}{\delta h} \right)^2 \right] \\ \frac{s_N}{1 - n_N/n_0} &= (2s + 1)N_f \frac{(2M\delta h)^{3/2}}{12} \left( \frac{T}{\delta h} \right), \end{aligned} \tag{17}$$

and for the quarks:

$$\begin{aligned}
n_Q &= (2s+1)N_f \frac{(2mh')^{3/2}}{6\pi^2} \left[ 1 + \frac{\pi^2}{8} \left( \frac{T}{h'} \right)^2 \right] \\
\epsilon_Q &= (2s+1)N_f N_c h' \frac{(2mh')^{3/2}}{10\pi^2} \left[ 1 + \frac{5\pi^2}{8} \left( \frac{T}{h'} \right)^2 \right] \\
s_Q &= (2s+1)N_f N_c \frac{(2mh')^{3/2}}{12} \left( \frac{T}{h'} \right), \tag{18}
\end{aligned}$$

where  $h' \equiv \frac{h-M}{N_c}$ . For clarity of notation, we use  $n_N$  and  $n_Q$  to denote the nucleon and quark densities, keeping in mind that we are interested in comparing the free energies of an all quark and an all nucleon configuration; at the end of the calculation we set  $n_N = n_Q = n_{tot}$ .

To obtain the free energy density as a function of  $n_N$  and  $n_Q$ , it is necessary to invert the shell radii in terms of the density and temperature, then substitute these relations into the energy and entropy densities. To lowest order, the shell radii read

$$\begin{aligned}
\delta h(T)/\delta h(0) &= 1 - \frac{\pi^2}{12} \left( \frac{T}{\delta h(0)} \right)^2 \\
h'(T)/h'(0) &= 1 - \frac{\pi^2}{12} \left( \frac{T}{h'(0)} \right)^2 \tag{19}
\end{aligned}$$

where  $\delta h(0) = \frac{1}{2M} \left( \frac{6\pi^2 n_N / (1-n_N/n_0)}{N_f(2s+1)} \right)^{2/3}$  and  $h'(0) = \frac{1}{2m} \left( \frac{6\pi^2 n_Q}{N_f(2s+1)} \right)^{2/3}$  are the standard zero temperature energies of free fermions. Eliminating the shell radii, one finds

$$\begin{aligned}
s_N &= (1 - n_N/n_0)^{2/3} M n_N^{1/3} T \left( \frac{(2s+1)\pi N_f}{6} \right)^{2/3} \\
s_Q &= m N_c n_Q^{1/3} T \left( \frac{(2s+1)\pi N_f}{6} \right)^{2/3} \tag{20}
\end{aligned}$$

and

$$\begin{aligned}
\epsilon_N &= \left( \frac{3}{5} \delta h(0) n_N \right) \left[ 1 + \frac{5}{3\pi^2} \left( \frac{(2s+1)\pi N_f}{6} \right)^{2/3} \frac{M^2 T^2}{(n_N / (1 - n_N/n_0))^{4/3}} \right] \\
\epsilon_Q &= \left( \frac{3}{5} N_c h'(0) n_Q \right) \left[ 1 + \frac{5}{3\pi^2} \left( \frac{(2s+1)\pi N_f}{6} \right)^{2/3} \frac{M^2 T^2}{n_Q^{4/3}} \right]. \tag{21}
\end{aligned}$$

Combing the energy and entropy, the change in the free energy for an all nucleon configuration due to the introduction of a temperature is

$$f_N(T) - f_N(0) = -\frac{1}{2} \left( 1 - \frac{n_N}{n_0} \right)^{2/3} M n_N^{1/3} T^2 \left( \frac{(2s+1)\pi N_f}{6} \right)^{2/3} \tag{22}$$

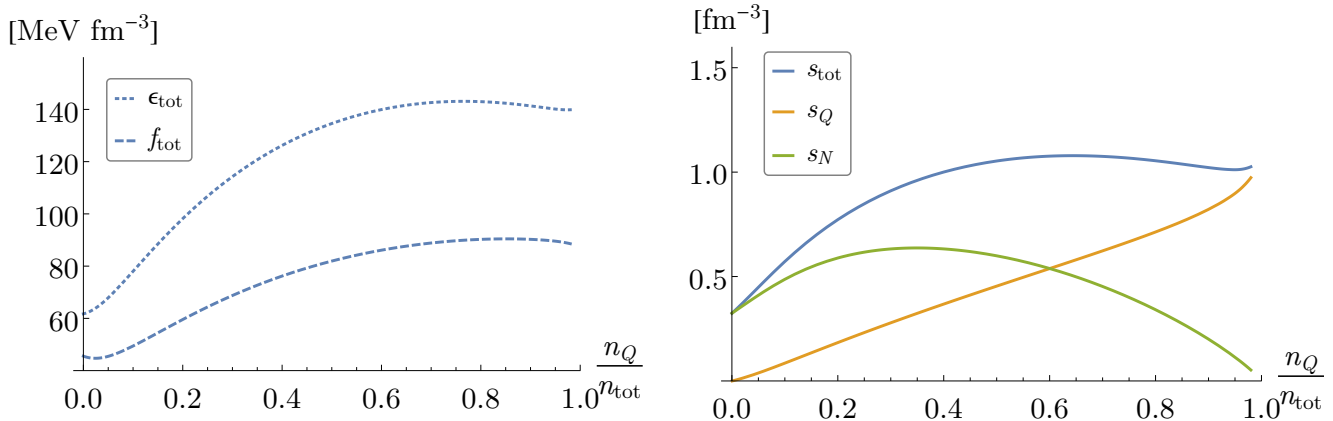


FIG. 5: Displayed are typical curves used in the minimization procedure. Here we have taken  $n_0 = 2.5n_{sat}$ ,  $T = 50$  MeV and  $n_{tot} = 2.2n_{sat}$ . The left panel shows the total energy and free energy densities as a function of quark fraction, while the right panel shows the individual and total entropies. The effect of entropy is to shift the minimum of the free energy from zero.

while the change in free energy for an all quark configuration is

$$f_Q(T) - f_Q(0) = -\frac{1}{2}Mn_Q^{1/3}T^2 \left( \frac{(2s+1)\pi N_f}{6} \right)^{2/3}. \quad (23)$$

Now setting  $n_N = n_Q = n_{tot}$ , the meaning of these free energy shifts becomes clear. The ratio of (the changes in) the free energy for the two configurations is

$$\frac{f_Q(T) - f_Q(0)}{f_N(T) - f_N(0)} = \frac{1}{(1 - n_{tot}/n_0)^{2/3}}. \quad (24)$$

Both species decrease in free energy as the temperature is increased, however the quarks decrease in energy faster than the nucleons. Therefore, while the case considered here is a simplification of the excluded volume model, it appears reasonable to conclude that more quarks will be produced at finite temperature than at zero temperature. This expectation is validated by our numerical calculations.

We now present our numerical results. In all that follows we take  $N_c = 3$ ,  $M = 938$  MeV,  $N_f = 2$  and  $s = 1/2$ . To begin, Fig. 5 illustrates a typical minimization procedure. Here the hard core density is set to  $2.5n_{sat}$ ,  $T = 50$  MeV and  $n_{tot} = 2.2n_{sat}$ . The left hand panel shows that, while the energy density  $\epsilon_{tot}$  has a minimum at zero quark fraction, the free energy density  $f_{tot}$  does not. This shift is due to entropy, shown on the right. As expected from the behavior of free particles, the entropy of quarks increases monotonically with quark

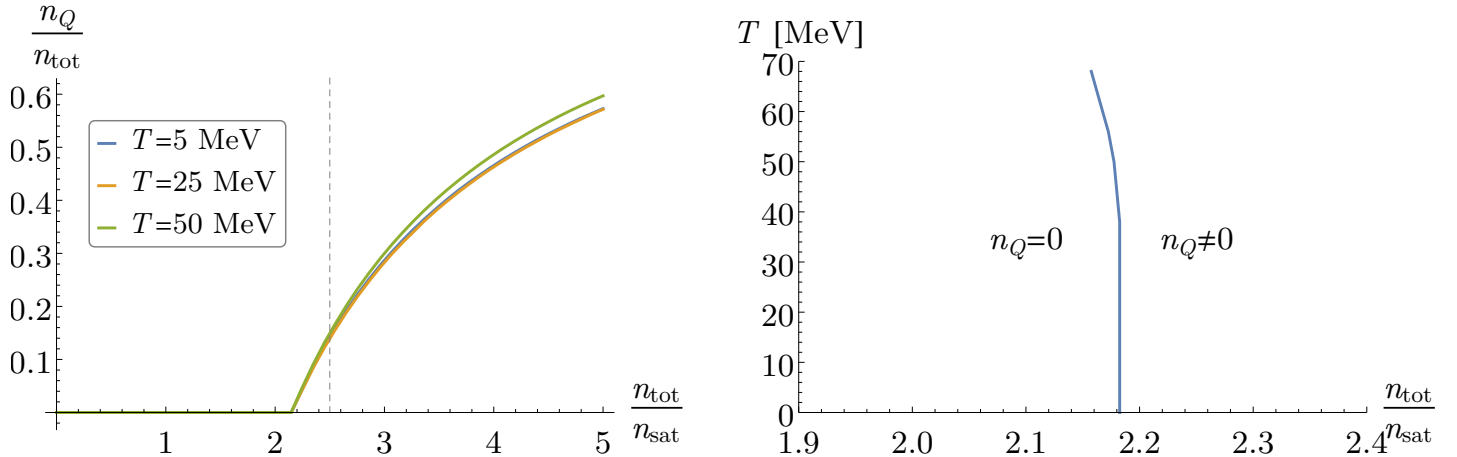


FIG. 6: Left: Here we plot the quark fraction  $n_Q/n_{tot}$  as a function of total density for a range of temperatures found in neutron star mergers. The vertical dashed line indicates the hard core density. It can be seen that, as the temperature is increased, quarks are produced in greater amount. Right: Plotted is the quark content of the excluded volume model in the temperature density plane with a hard core density of  $2.5n_{sat}$ . The onset density is largely insensitive to temperature decreasing slightly with increasing temperature under neutron star merger conditions.

fraction. This is not the case with nucleons, where the maximum entropy occurs at a quark fraction of  $\sim 30\%$ . This non-trivial behavior is due to the competition between increasing density and the excluded volume factor  $(1 - n/n_0)$ .

Next, in Fig. 6 we plot the quark fraction for a range of thermodynamic conditions. In particular, we choose temperatures and densities expected in neutron star mergers [12], and once again the hard core density is taken to be  $n_0 = 2.5n_{sat}$ . Several features of the excluded volume model can be gleaned from Fig. 6. First, as expected from the low temperature expansion, quarks appear at lower density and in greater amount as the temperature is raised. Second, the onset density changes by only  $\sim 2\%$  over the temperature range examined. This robustness of the onset density, while perhaps surprising, can be simply understood: quarks, residing within the shell of nucleons, are largely protected from the temperature. Indeed, at the onset density the distribution function is nearly all “shell”, and large temperatures are required to deform the fermi surface enough to affect quarks. The low temperature expansion can be used to substantiate this claim. To do so, note the system is nearly all nucleons

at the onset density, so we can safely neglect quarks. Now, the factor  $(1 - n/n_0)^{-1/3} \sim N_c$  near the onset density, so the free energy shifts by an amount

$$\frac{f_N(T) - f_N(0)}{f_N(0)} = \frac{10}{9} \left( \frac{2}{3\pi^2} \right)^{1/3} \left( \frac{MT}{n^{2/3} N_c^2} \right)^2. \quad (25)$$

at temperature is  $T$ . At  $T = 50$  MeV and  $n = 2.5n_{sat}$ ,  $(f_N(T) - f_N(0))/f_N(0) \sim 3\%$ , which is close to the exact shift of  $\sim 2\%$ . Interestingly, the estimate Eq. 25 reveals that  $N_c$  factors are what cause the system be insensitive to temperature. Indeed, dimensional analysis alone would dictate that the shift in the onset density is  $(f_N(T) - f_N(0))/f_N(0) \sim \left( MT/n^{2/3} \right)^2$ , which is well beyond  $\mathcal{O}(1)$  when  $T = 50$  MeV.

In the right panel of Fig. 6, we demarcate the quark content in various regions in the of the temperature/density plane. Within the model, we conclude that the effect of temperature is to slightly decrease the onset density relative to the zero temperature case. Whether this prediction of the excluded volume model extends to reality is not known, and must be checked by more microscopic calculations. Finally, varying the single parameter of this model, the hard core density, we find that the quark onset density is well approximated by the simple relation  $n_{onset} = 0.863n_0$ , correct to 5%, for temperatures between  $0 \text{ MeV} \leq T \leq 50 \text{ MeV}$ .

## V. CONCLUSION

In this paper we studied the finite temperature properties of an excluded volume model of quarkyonic matter. To do so, we introduced finite temperature distribution functions and entropy functionals motivated by the momentum-space shell structure of [5, 7]. Due to entropy, we find that the quark onset happens at lower densities at finite temperature than at zero temperature. Additionally, for a fixed density, we find that the amount of quarks produced increases as a function of temperature. If a nuclear to quark matter transformation behaves as suggested by this model, it would imply that relatively hot environments such as neutron stars mergers are more likely to carry signatures of quark matter than zero temperature environments.

We conclude by noting that, with finite temperature distribution functions and a complete set of thermodynamic functionals in hand, it is possible to compute in the excluded volume model a number of observables relevant to nuclear astrophysics. For example, the finite temperature equation of state as well as the speed of sound of quarkyonic matter can be

computed. It may also be useful to compute mass-radius relations of neutron stars in the excluded volume model to compare with the constraints of [8, 23], where a peak in the sound velocity between  $2 - 3n_{sat}$  is favored. Finally, using finite-temperature distribution functions extracted from the excluded volume model, neutrino scattering rates through hot, dense merger matter may be computed.

## VI. ACKNOWLEDGEMENTS

N.C.W. is grateful to Sanjay Reddy and Larry McLerran for their constructive comments. The work of N.C.W. was supported by U.S. DOE under Grant No. DE-FG02-00ER41132. The work of S.S. was supported by Iowa State University Startup funds.

- 
- [1] Larry McLerran and Robert D. Pisarski. Phases of cold, dense quarks at large  $N(c)$ . *Nucl. Phys.*, A796:83–100, 2007.
  - [2] Toru Kojo, Yoshimasa Hidaka, Larry McLerran, and Robert D. Pisarski. Quarkyonic Chiral Spirals. *Nucl. Phys.*, A843:37–58, 2010.
  - [3] Elias R. Most, L. Jens Papenfort, Veronica Dexheimer, Matthias Hanauske, Stefan Schramm, Horst Stöcker, and Luciano Rezzolla. Signatures of quark-hadron phase transitions in general-relativistic neutron-star mergers. *Phys. Rev. Lett.*, 122:061101, Feb 2019.
  - [4] Roland Oechslin, K. Uryu, Gevorg S. Poghosyan, and F. K. Thielemann. The Influence of quark matter at high densities on binary neutron star mergers. *Mon. Not. Roy. Astron. Soc.*, 349:1469, 2004.
  - [5] Larry McLerran and Sanjay Reddy. Quarkyonic Matter and Neutron Stars. *Phys. Rev. Lett.*, 122(12):122701, 2019.
  - [6] Kenji Fukushima and Toru Kojo. The Quarkyonic Star. *Astrophys. J.*, 817(2):180, 2016.
  - [7] Kie Sang Jeong, Larry McLerran, and Srimoyee Sen. Dynamical Derivation of the Momentum Space Shell Structure for Quarkyonic Matter. 2019.
  - [8] I. Tews, J. Carlson, S. Gandolfi, and S. Reddy. Constraining the speed of sound inside neutron stars with chiral effective field theory interactions and observations. *The Astrophysical Journal*, 860(2):149, jun 2018.

- [9] Katerina Chatziioannou and Sophia Han. Studying strong phase transitions in neutron stars with gravitational waves. 2019.
- [10] Andreas Bauswein, Niels-Uwe F. Bastian, David B. Blaschke, Katerina Chatziioannou, James A. Clark, Tobias Fischer, and Micaela Oertel. Identifying a first-order phase transition in neutron star mergers through gravitational waves. *Phys. Rev. Lett.*, 122(6):061102, 2019.
- [11] Paul M. Chesler, Niko Jokela, Abraham Loeb, and Alekski Vuorinen. Finite-temperature equations of state for neutron star mergers. *Phys. Rev. D*, 100:066027, Sep 2019.
- [12] Albino Perego, Sebastiano Bernuzzi, and David Radice. Thermodynamics conditions of matter in neutron star mergers. *The European Physical Journal A*, 55(8):124, 2019.
- [13] K.E. Schmidt and S. Fantoni. A quantum monte carlo method for nucleon systems. *Physics Letters B*, 446(2):99 – 103, 1999.
- [14] D. Lonardonì, S. Gandolfi, J. E. Lynn, C. Petrie, J. Carlson, K. E. Schmidt, and A. Schwenk. Auxiliary field diffusion monte carlo calculations of light and medium-mass nuclei with local chiral interactions. *Phys. Rev. C*, 97:044318, Apr 2018.
- [15] J. Carlson, S. Gandolfi, F. Pederiva, Steven C. Pieper, R. Schiavilla, K. E. Schmidt, and R. B. Wiringa. Quantum monte carlo methods for nuclear physics. *Rev. Mod. Phys.*, 87:1067–1118, Sep 2015.
- [16] Philippe de Forcrand. Simulating QCD at finite density. *PoS*, LAT2009:010, 2009.
- [17] V. G. J. Stoks, R. A. M. Klomp, M. C. M. Rentmeester, and J. J. de Swart. Partial-wave analysis of all nucleon-nucleon scattering data below 350 mev. *Phys. Rev. C*, 48:792–815, Aug 1993.
- [18] Evgeny Epelbaum, Hans-Werner Hammer, and Ulf-G. Meissner. Modern Theory of Nuclear Forces. *Rev. Mod. Phys.*, 81:1773–1825, 2009.
- [19] Note that the baryon number of a single quark is  $1/N_c$  and that there are  $N_c$  species of quarks in our theory. These facts lead to non-trivial cancellations in the thermodynamic functionals.
- [20] H.B. Callen. *THERMODYNAMICS*. 1960.
- [21] David Radice, Sebastiano Bernuzzi, Walter Del Pozzo, Luke F. Roberts, and Christian D. Ott. Probing Extreme-Density Matter with Gravitational Wave Observations of Binary Neutron Star Merger Remnants. *Astrophys. J.*, 842(2):L10, 2017.



- [22] A. Sommerfeld. Zur elektronentheorie der metalle auf grund der fermischen statistik. *Zeitschrift für Physik*, 47(1):1–32, 1928.
- [23] Collin D. Capano, Ingo Tews, Stephanie M. Brown, Ben Margalit, Soumi De, Sumit Kumar, Duncan A. Brown, Badri Krishnan, and Sanjay Reddy. GW170817: Stringent constraints on neutron-star radii from multimessenger observations and nuclear theory. 2019.